

Dispersion and Stability Studies of Resorcinarene-Encapsulated Gold Nanoparticles

R. Balasubramanian,[†] Beomseok Kim,[†] Steven L. Tripp,[†] Xuejun Wang,[‡]
Marya Lieberman,^{*,‡} and Alexander Wei^{*,†}

Department of Chemistry, Purdue University, West Lafayette, Indiana 47907-1393, and
Department of Chemistry and Biochemistry, University of Notre Dame,
Notre Dame, Indiana 46556

Received October 3, 2001. In Final Form: February 4, 2002

Two resorcinarene surfactants with sulfur-functionalized headgroups have been evaluated for their ability to stabilize dispersions of midnanometer (16–87 nm)-sized gold particles in organic solvents. Citrate-stabilized colloidal gold nanoparticles were extracted from aqueous solutions into toluene or chloroform by tetrabenzylthiol resorcinarene **1** or tetraarylthiol resorcinarene **2**. The nanoparticle dispersions were subjected to various conditions and monitored for changes in plasmon absorption intensity. The stability of the dispersions was dependent on the chemisorptive properties of the surfactant headgroup, with tetrabenzylthiol **1** being the more effective dispersant. Nanoparticles encapsulated by **1** were also highly robust, demonstrated good resistance to alkanethiol-induced flocculation, and could be redispersed after repeated precipitations in polar solvents. Surface-enhanced Raman scattering analysis and X-ray photoelectron spectroscopic studies confirmed significant differences in the chemisorptive properties of tetrathioles **1** and **2**, indicating that surface passivation is an important factor in the dispersibility of colloidal gold nanoparticles in nonpolar solvents.

Introduction

The chemistry and physics of metallic nanoparticles have been a topic of enduring interest since Faraday's seminal insights into the optical properties of colloidal gold.¹ Metal nanoparticles are presently used in a wide range of applications such as catalysis,² optical labeling,³ ferrofluids,⁴ and sensing.⁵ These applications, along with the recent attention to nanoscale science and technology, fuel the demand for methodologies which enable nanoparticles to be incorporated into nanostructured devices and composite materials. Dispersing metal particles in nonpolar organic solvents is appealing because the low interfacial energies should allow for a high degree of control during solution and surface processing. Unbranched alkanethiols and carboxylic acids have been used to stabilize dispersions of small (<10 nm) metal nanoparticles in organic solvents,⁶ but encapsulated particles above this size threshold are often prone to flocculation because the steric repulsive forces are overwhelmed by the increase in van der Waals attraction.^{7,8} The robustness of the

surfactant layer can also have an important role in the stability of the nanoparticle dispersions, which is determined by the rate of desorption or displacement of the surfactant molecules from the metal surface.⁹ The relative ease with which chemisorbed ligands can be displaced is an impediment to the development of metal nanoparticles as substrates in chemical and biotechnological applications.¹⁰

To increase the size range of metal nanoparticles which can be dispersed in nonpolar solvents, attractive interparticle forces must be countered by greater short-range repulsion by designing surfactant layers with high conformational entropy. Many polymeric surfactants are excellent dispersants because of their elasticities;¹¹ however, such coatings on nanoparticles are often nonuniform or are poorly suited for applications requiring monolayer thickness. On the other hand, single-chain monodentate surfactants (e.g., *n*-alkanethiols) are generally poor dispersants because of their tendency to pack densely with crystalline order.¹² Introducing disorder into the surfactant barrier increases repulsion entropically; for example, kinked surfactants such as oleic acid have been used to enhance the dispersion of magnetic nanoparticles.¹³ Alternatively, increasing the spacing between chains

[†] Purdue University.

[‡] University of Notre Dame.

(1) Faraday, M. *Philos. Trans. R. Soc. London* **1857**, 147, 145.

(2) Bönemann, H.; Brijoux, W. In *Advanced Catalysts and Nanostructured Materials*; Moser, W. R., Ed.; Academic Press: San Diego, 1996; pp 165–96.

(3) *Colloidal Gold: Principles, Methods, and Applications*; Hayat, M. A., Ed.; Academic Press: San Diego, 1989; Vol. 1.

(4) Rankin, P. J.; Ginder, J. M.; Klingenberg, D. J. *Curr. Opin. Colloid Interface Sci.* **1998**, 3, 373–81.

(5) (a) Elghamian, R.; Storhoff, J. J.; Mucic, R. C.; Letsinger, R. L.; Mirkin, C. A. *Science* **1997**, 277, 1078–81. (b) Wohltjen, H.; Snow, A. W. *Anal. Chem.* **1998**, 70, 2856–59. (c) Wei, A.; Kim, B.; Tripp, S. L. *ChemPhysChem*, in press.

(6) (a) Brust, M.; Fink, J.; Bethell, D.; Schiffrin, D. J.; Kiely, C. J. *Chem. Soc., Chem. Commun.* **1995**, 1655–56. (b) Templeton, A. C.; Hostetler, M. J.; Kraft, C. T.; Murray, R. W. *J. Am. Chem. Soc.* **1998**, 120, 1906–11. (c) Sarathy, K. V.; Kulkarni, G. U.; Rao, C. N. R. *Chem Commun.* **1997**, 537–38.

(7) (a) Israelachvili, J. *Intermolecular and Surface Forces*, 2nd ed.; Academic Press: New York, 1992; Chapter 10. (b) Evans, D. F.; Wennerström, H. *The Colloidal Domain. Where Physics, Chemistry, Biology, and Technology Meet*, 2nd ed.; Wiley-VCH: New York, 1999.

(8) Metal nanoparticles possess planar facets which also increase with particle size such that the interactions are between flat rather than curved surfaces, contributing further to the van der Waals attraction.

(9) Schlenoff, J. B.; Li, M.; Ly, H. *J. Am. Chem. Soc.* **1995**, 117, 12528–36.

(10) (a) Yguerabide, J.; Yguerabide, E. E. *Anal. Biochem.* **1998**, 262, 157–76. (b) West, J. L.; Halas, N. J. *Curr. Opin. Biotechnol.* **2000**, 11, 215–17. (c) Taton, T. A.; Lu, G.; Mirkin, C. A. *J. Am. Chem. Soc.* **2001**, 123, 5164–65.

(11) Napper, D. H. *Polymeric Stabilization of Colloidal Dispersions*; Academic Press: London, 1983.

(12) (a) Dubois, L. H.; Nuzzo, R. G. *Annu. Rev. Phys. Chem.* **1992**, 43, 437–63. (b) Badia, A.; Cuccia, L.; Demers, L.; Morin, F.; Lennox, R. B. *J. Am. Chem. Soc.* **1997**, 119, 2682–92.

(13) (a) Suslick, K. S.; Fang, M.; Hyeon, T. *J. Am. Chem. Soc.* **1996**, 118, 11960–61. (b) Shafi, K. V. P. M.; Gedanken, A.; Prozorov, R. *Adv. Mater.* **1998**, 10, 590–93.

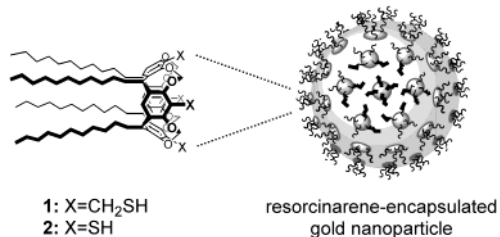


Figure 1. Gold nanoparticle encapsulated by tetrathiolated resorcinarene **1** ($R=CH_2SH$) or **2** ($R=SH$).

should greatly increase the overall conformational entropy of the surfactant layer.

We have been investigating the latter approach to nanoparticle dispersion using a class of macrocyclic compounds known as resorcinarenes.¹⁴ These molecules differ from conventional short-chain surfactants in several regards: (i) their large macrocyclic headgroups require fewer surfactant molecules per unit area, reducing the entropic cost of encapsulation; (ii) their adsorption to the nanoparticle surface can be greatly stabilized by cooperative, multidentate interactions; and (iii) the macrocyclic base can be appended by several hydrocarbon tails at fixed spacings. This last feature ensures that the hydrocarbon chains will always possess a certain degree of conformational freedom, regardless how densely packed the resorcinarene headgroups are on the nanoparticle surface.

Here we describe the dispersant properties of two resorcinarene-derived surfactants with sulfur-functionalized headgroups, tetrabenzylthiol C11 resorcinarene (**1**) and tetraarylthiol C11 resorcinarene (**2**) (see Figure 1). These thiolated resorcinarenes enable the extraction and dispersion of colloidal gold particles up to nearly 100 nm from aqueous solutions into nonpolar organic solvents. Compound **1** is an especially effective dispersant and provides a coating which is resistant to degradation by competing surfactants. Surfactant layers of **1** also enhance the robustness of encapsulated nanoparticles against repeated cycles of precipitation and redispersion.

Experimental Section

Materials. Resorcinarenes were synthesized by adaptation of known synthetic procedures.¹⁵ Tetrabenzylthiol **1** was synthesized by O,O-methylenation of tetra(2-methyl)resorcinarene at elevated temperature and pressure,¹⁶ followed by bromination of the methyl groups¹⁷ and treatment with thiourea.¹⁸ Tetraarylthiol **2** was prepared by lithium-halogen exchange of the corresponding tetrabromide¹⁹ followed by treatment with elemental sulfur.²⁰ Dodecanethiol and propanethiol were purchased from Aldrich and used without further purification. Gold particles (19 nm) were prepared by the reduction of gold chloride with sodium citrate^{3,21} (estimated concentration $\sim 2 \times 10^{12}$ particles/mL); larger sized particles were purchased from British Biocell International. All gold colloid solutions were analyzed by transmission electron microscopy (TEM); particle batches with size dispersities of 10–15% were used without further purification.

(14) (a) Stavens, K. B.; Pusztay, S. V.; Zou, S.; Andres, R. P.; Wei, A. *Langmuir* **1999**, *15*, 8337–39. (b) Balasubramanian, R.; Xu, J.; Kim, B.; Sadtler, B.; Wei, A. *J. Dispersion Sci. Technol.* **2001**, *22*, 485–89.

(15) Selected synthetic procedures and chemical characterization of these compounds are reported in the Supporting Information.

(16) Román, E.; Peinador, C.; Mendoza, S.; Kaifer, A. E. *J. Org. Chem.* **1999**, *64*, 2577–78.

(17) Sorrell, T. N.; Pigge, F. C. *J. Org. Chem.* **1993**, *58*, 784–85.

(18) Cram, D. J.; Karbach, S.; Kim, Y. H.; Baczynskyj, L.; Kallemeyn, G. W. *J. Am. Chem. Soc.* **1985**, *107*, 2575–76.

(19) Timmerman, P.; Nierop, K. G. A.; Brinks, E. A.; Verboom, W.; van Veggel, F. C. J. M.; van Hoorn, W. P.; Reinhoudt, D. N. *Chem.-Eur. J.* **1995**, *1*, 132–43.

(20) Gibb, B. C.; Mezo, A. R.; Causton, A. S.; Fraser, J. R.; Tsai, F. C. S.; Sherman, J. C. *Tetrahedron* **1995**, *51*, 8719–32.

(21) Frens, G. *Nature (London), Phys. Sci.* **1973**, *241*, 20–22.

General Procedures. *Extraction of Gold Colloid into Organic Solvents.* All glassware and cuvettes were silanized (Siliclad, Gel-Est) during the handling of resorcinarene-encapsulated gold particles to minimize surface adsorption. Conditions for extracting gold nanoparticles were typically performed as follows: an aqueous suspension of Au colloid (4 mL) was vigorously mixed in a silanized test tube with an equal volume of a 1–2 mM solution of resorcinarene in tetrahydrofuran (THF). A 10 μ M solution of tetra-*n*-octylammonium bromide (TOAB) in toluene (4 mL) was then added, and the mixture was vigorously agitated for 30 s using a vortex mixer. Extractions without TOAB generally resulted in only partial transfer of the Au nanoparticles into the organic phase. The organic layer was separated using a silanized pipet and dried for 2 h over prewashed 4A molecular sieves. THF could be removed by distillation using a rotary evaporator; extracts were diluted 10-fold with toluene and concentrated to their original volume twice. In the case of 19-nm gold particles, the dispersions in their final state had absorbances at 532 nm between 0.14 and 0.20, with surfactant concentrations between 1.0 and 1.5 mM.

Dispersion and Particle Stability Studies. Changes in optical absorbance (extinction) were monitored at room temperature using a Cary 300 Bio spectrophotometer with a spectral resolution of 1 nm. Silanized cuvettes were handled with minimal disturbance to prevent the redispersion of precipitated particles. TEM analysis of the particles suspended in toluene was performed with a Philips EM-400 with an accelerating voltage of 80 kV using Formvar-coated Cu grids. Solvent-induced precipitations were performed by the concentration of 19-nm particles suspended in toluene to minimal volume (0.1–0.2 mL) followed by the addition of reagent-grade MeOH (7–8 mL). The precipitates were collected by centrifugation at 1000, 3000, or 11000 rpm for 20 min in heavy-walled conical vials and then decanted from the supernatant and redispersed in toluene to their original volumes by a swirling motion.

Surface-Enhanced Raman Scattering (SERS) and X-ray Photoelectron Spectroscopic (XPS) Studies. Raman spectra were acquired in backscattering geometry at an excitation wavelength of 785 nm, using a home-built imaging microscope with a 40 \times objective lens (Olympus, NA = 0.75) and a charge-coupled device camera (resolution = 2 cm⁻¹).²² Samples were exposed for 30 s to a laser power of 10 mW. SERS samples were prepared by extracting encapsulated 42-nm gold particles from aqueous-THF solutions using toluene in the absence of TOAB. Nanoparticulate thin films were formed at the air–water interface and transferred onto quartz substrates using a mechanically controlled deposition arm (Kibron, Inc.).²³ XPS spectra were obtained using a Kratos Analytical ESCA system with monochromatic Al K α radiation at 1486.6 eV and a fixed takeoff angle of 90°. Monolayers of **1** and **2** were prepared by immersing freshly cleaned Au(111) surfaces in 1 mM solutions of tetrathiol in 3:1 EtOH/CHCl₃ for 16 h at room temperature and then thoroughly washed with solvent. Monolayers and powder samples were mounted using conductive carbon tape. Binding energies for S were referenced to the Au 4f_{7/2} peak at 84.0 eV; S 2p_{3/2} and 2p_{1/2} peaks were fitted to the raw spectra with 70% Gaussian/30% Lorentzian peaks using Kratos Vision II software as previously described.²⁴ Peak positions are reported here as that of the 2p_{3/2} component.

Results and Discussion

Resorcinarenes **1** and **2** and dodecanethiol were all effective at extracting 5-nm colloidal gold particles into hexanes, toluene, or chloroform without requiring phase-transfer reagents. However, their abilities to extract and disperse larger (> 19 nm) particles were highly variable. Dodecanethiol was a poor dispersant; 19-nm particles could be partially extracted into THF–chloroform, but the purplish tint and short lifetime (<5 days) of these

(22) Gift, A. D.; Ma, J. Y.; Haber, K. S.; McClain, B. L.; Ben-Amotz, D. *J. Raman Spectrosc.* **1999**, *30*, 757–65.

(23) (a) Kim, B.; Tripp, S. L.; Wei, A. *J. Am. Chem. Soc.* **2001**, *123*, 7955–56. (b) Wei, A.; Kim, B.; Sadtler, B.; Tripp, S. L. *ChemPhysChem* **2001**, *2*, 743–45.

(24) Li, Z.; Lieberman, M.; Hill, W. *Langmuir* **2001**, *17*, 4887–94.

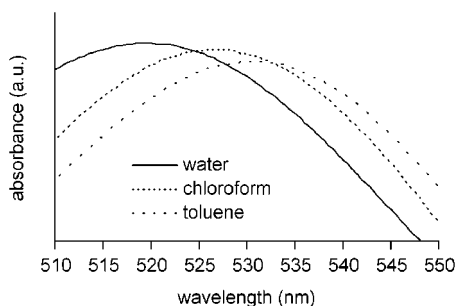


Figure 2. Optical extinction spectra of 19-nm colloidal gold particles dispersed in water ($n = 1.333$), chloroform ($n = 1.446$), and toluene ($n = 1.496$).

dispersions indicated that the dodecanethiol-coated particles flocculated rapidly under these conditions. Resorcinarenes **1** and **2** were far more effective at nanoparticle extraction and dispersion into THF–toluene and THF–chloroform, but their efficacies varied widely between experiments. TOAB greatly increased the efficiency and reproducibility of phase transfer, with < 5 mol % of TOAB per equivalent of surfactant being sufficient in most cases. The tetraalkylammonium cation presumably exchanges with the inorganic counterions in the electrostatic double layer, increasing the hydrophobic character of the encapsulated nanoparticles.

Fully dispersed gold colloid solutions produced a red or pink color characteristic of the particles' surface plasmon excitations. Optical extinction spectra of 19-nm gold particles stabilized by **1** or **2** in different solvents revealed redshifts in the plasmon resonance peak relative to aqueous dispersions. The plasmon resonances increased linearly with the solvent refractive index (see Figure 2), in accord with earlier observations on the optical responses of polymer-stabilized gold particles dispersed in non-aqueous solutions.²⁵ Particles encapsulated by **1** in toluene which had been exposed to alkanethiol (see below) exhibited a slight (~ 1 nm) blueshift in plasmon resonance, possibly due to changes in surface passivation.²⁶

Tetraarylylthiol **1** proved to be the more effective dispersant and could extract and stabilize colloidal gold nanoparticles up to 42 nm into 1:1 THF/toluene and up to 70 nm into 1:1 THF/chloroform in the presence of a small amount of TOAB (0.5–3 mol % depending on the particle size). In many cases, the dispersions were stable for several weeks at ambient temperature with minimal changes in extinction intensity or wavelength. Colloidal gold particles up to 87 nm could be reproducibly extracted into chloroform with **1** when mediated by higher concentrations of TOAB (20–25 mol %); however, suspensions of these particles were somewhat less stable, losing their tint after several days. Tetraarylylthiol **2** was less effective at extracting gold colloid in comparison to **1** and was able to extract 19-nm particles into THF–toluene and 42-nm particles into THF–chloroform in the presence of 0.5 and 5 mol % of TOAB, respectively. Increasing the TOAB concentration did not improve extraction efficiency and often resulted instead in emulsion formation. The difference in dispersion efficacy of **1** and **2** is most likely related to the surfactants' chemisorptive properties (see below); well-passivated colloids should bear less surface charge and transfer more readily into nonpolar media, given sufficient steric stabilization.

(25) Underwood, S.; Mulvaney, P. *Langmuir* **1994**, *10*, 3427–30.

(26) A comprehensive treatise by Mulvaney discusses the damping effect of chemisorptive ligands on the surface plasmon frequencies of metal nanoparticles: Mulvaney, P. *Langmuir* **1996**, *12*, 788–800.

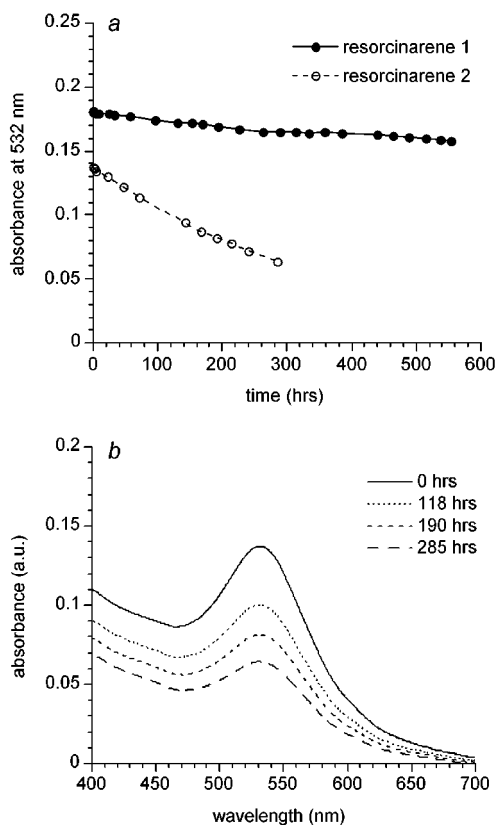


Figure 3. (a) Dispersion stability of 19-nm gold particles encapsulated by **1** (circles, filled) or **2** (circles, open) in toluene at 25 °C, monitored by their surface plasmon maxima of 532 nm. (b) Optical extinction spectra of 19-nm gold particles stabilized by **2** over time.

The resorcinarene-stabilized colloid dispersions were monitored for changes in optical extinction over time. Dispersions of 19-nm gold particles stabilized by tetraarylylthiol **1** in toluene or chloroform experienced less than a 10% drop in extinction over a period of 4 weeks (see Figure 3a). The same-sized nanoparticles encapsulated by tetraarylylthiol **2** were less stable by comparison: the dispersion half-life (defined here as the time elapsed for the optical density to decrease by 50%) of these particles in toluene was approximately 1.5 weeks. Examination of spectra revealed no significant increases in extinction at wavelengths above 600 nm, demonstrating that the particles stabilized by **2** did not form an intermediate flocculated state in solution over time (see Figure 3b).

THF was important for stabilizing the larger nanoparticle dispersions in organic solvents. In the case of 19-nm particles extracted into toluene by **1**, long-term dispersion stability was not significantly affected by removing THF. However, for larger colloidal particles (> 40 nm) extracted into toluene or chloroform, long-term dispersion stability was greatly enhanced by the presence of THF. Attempts to remove THF from these dispersions usually resulted in flocculation within 24 h, as indicated by a decrease or redshift in optical extinction.²⁷

The resorcinarene-encapsulated nanoparticles were evaluated for their robustness against flocculation or degradation by competing alkanethiol surfactants. Dispersions of weakly passivated gold particles in hydrocarbon solvents have been shown to be destabilized by the addition of alkanethiol.^{14a} Dispersions of 19-nm gold particles encapsulated by **1** (1 mM) in toluene or THF–

(27) Weisbecker, C. S.; Merritt, M. V.; Whitesides, G. M. *Langmuir* **1996**, *12*, 3763–72.

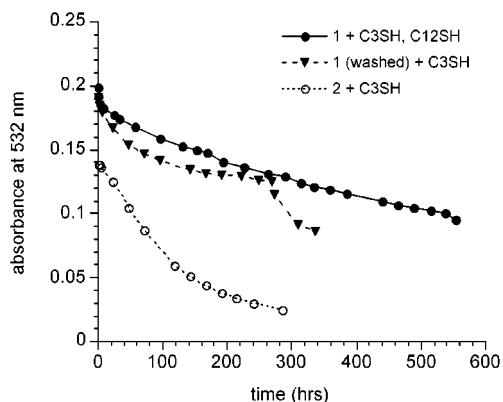


Figure 4. Dispersion stability of resorcinarene-encapsulated 19-nm gold particles in the presence of competing alkanethiol surfactants. Circles (filled): gold nanoparticles stabilized by **1** in toluene at 25 °C in the presence of **1** (1.5 mM) and propanethiol (C3SH, 1.7 mM); after 170 h, the dispersion was treated with additional dodecanethiol (C12SH, 1.7 mM). Triangles: gold nanoparticles stabilized by **1** washed twice with hexanes and then dispersed in toluene at 25 °C in the presence of C3SH (1.7 mM); after 215 h, the dispersion was treated with additional C12SH (5.6 mM); after 265 h, the dispersion was heated to 70 °C for 2 h. Circles (open): gold nanoparticles stabilized by **2** in toluene at 25 °C in the presence of **2** (1.5 mM) and C3SH (1.7 mM).

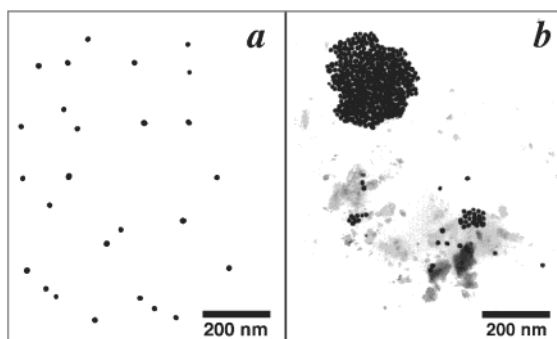


Figure 5. Transmission electron micrographs (Philips EM-400, 80 keV) of 19-nm colloidal gold particles stabilized by **1** in the absence (a) and presence (b) of propanethiol. Nanoparticles were dispersed in toluene, aged for 6 weeks, and then dropped onto Formvar-coated Cu grids (300 mesh) and dried by slow evaporation in air. Organic deposits are evident in the propanethiol-treated sample.

toluene were quite robust in the presence of either propanethiol or dodecanethiol (3.5–7.5 mM), with a half-life of over 3 weeks (550 h) at room temperature (see Figure 4). Dispersions of 40-nm gold particles encapsulated by **1** in THF–toluene were much less stable; treatment of these particles with dodecanethiol led to nearly complete flocculation within 24 h. Finally, the stability of 19-nm gold particles in toluene encapsulated by **2** (1 mM) against alkanethiol-induced precipitation was inferior to those stabilized with **1**; the half-life was observed to be just over 4 days (100 h) at room temperature in the presence of 1.7 mM propanethiol.

Transmission electron microscopy revealed that prolonged exposure of the resorcinarene-encapsulated nanoparticles to alkanethiols increased their tendency to flocculate upon drying, suggesting partial degradation of the resorcinarene surfactant layer (see Figure 5). However, varying the alkanethiol concentration from 1 to 7.5 mM did not visibly affect the rate of degradation for 19-nm particles stabilized by **1** in toluene. Lowering the resorcinarene concentration by washing encapsulated gold particles twice with hexanes prior to extraction into

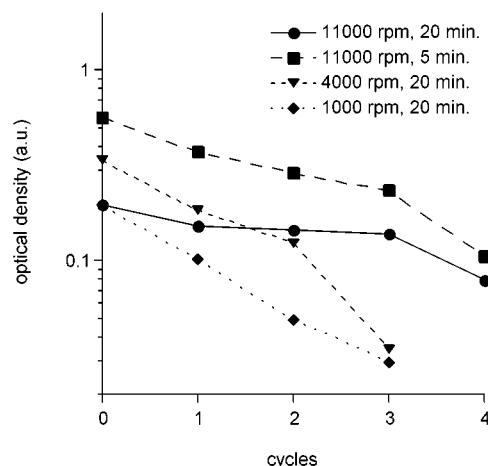


Figure 6. Semilogarithmic plot of optical densities of 19-nm gold particles encapsulated by **1** as a function of solvent-induced precipitation–redispersion cycles. Nanoparticle dispersions were concentrated, flocculated in methanol and centrifuged, and then decanted and redispersed in toluene. Optical densities were recorded at the extinction maxima at the end of each cycle. Centrifugations were performed at 11000 rpm for 20 min (circles), 11000 rpm for 5 min (squares), 3000 rpm for 20 min (triangles), and 1000 rpm for 40 min (diamonds).

toluene and treatment with propanethiol also did not result in increased flocculation or degradation. On the other hand, heating the dispersions to 70 °C for 2 h accelerated degradation considerably (see Figure 4). The effect of temperature on dispersion stability clearly indicated that (i) nanoparticle degradation could be correlated with the displacement of the resorcinarene surfactants by the alkanethiols and (ii) the rate of surfactant exchange in toluene on the nanoparticle surfaces was extremely slow at room temperature.

Nanoparticles encapsulated by **1** were also evaluated for their robustness against degradation by solvent-induced precipitation. Dispersions of 19-nm particles were repeatedly flocculated in MeOH, centrifuged at 11000 rpm for 20 min, and then decanted and redispersed to their original volumes in toluene. The resorcinarene-encapsulated nanoparticles demonstrated moderate stability to precipitation/redispersion, with approximately 80% of the optical density recovered after each cycle on average (see Figure 6). Lower rotor speeds and shorter centrifugation times did not improve redispersion; in fact, decreasing centrifugal force resulted in greater loss of optical density, possibly due to incomplete precipitation and loss of nanoparticles upon decanting. Strategies for cross-linking the surfactant layer have been recently demonstrated²⁸ and may be useful for further increasing the robustness of the encapsulated nanoparticles.

SERS and XPS analyses were performed to determine whether the efficacies of **1** and **2** as dispersants could be correlated with their bonding to Au. Surface-enhanced Raman spectra of encapsulated nanoparticles and powder Raman spectra of the tetrathiol surfactants were obtained at 785 nm laser excitation (see Figure 7). In the case of tetrabenzylthiol **1**, an intense SERS peak was observed at 300 cm⁻¹ with a shoulder at roughly 250 cm⁻¹. This peak is not present in the powder spectrum of **1** and is almost certainly associated with $\nu_{\text{Au-S}}$, a well-characterized stretching mode for alkanethiols on roughened Au sur-

(28) (a) Wu, M. L.; O'Neill, S. A.; Brousseau, L. C.; McConnell, W. P.; Shultz, D. A.; Linderman, R. J.; Feldheim, D. L. *Chem. Commun.* **2000**, 775–76. (b) Pusztay, S. V.; Wei, A.; Stavens, K. B.; Andres, R. P. *Supramol. Chem.* **2002**, *14*, 289–292.

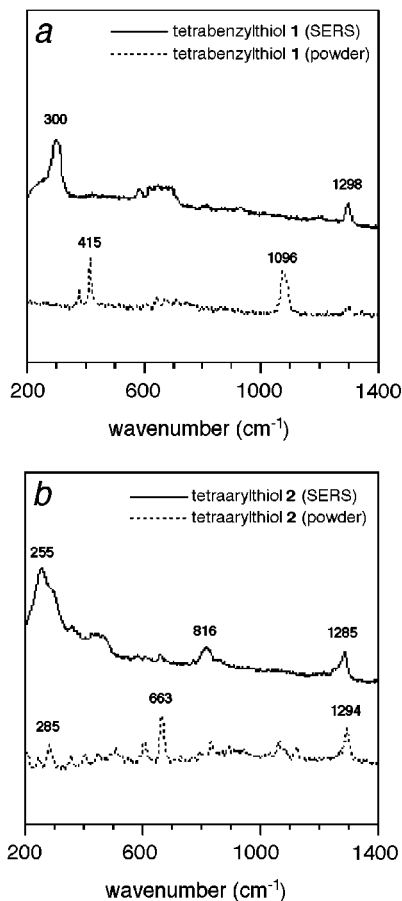


Figure 7. Surface-enhanced and powder Raman spectra of **1** and **2**. Spectra were acquired using a micro-Raman spectrometer operating at 785 nm with a 40 \times objective lens (NA = 0.75), an input power of 10 mW at the sample, and an exposure time of 30 s. (a) Tetrabenzylthiol **1** adsorbed onto 40-nm Au particles (—) and in powder form (---); (b) tetraarylthiol **2** adsorbed onto 40-nm Au particles (—) and in powder form (---). Spectra have been shifted for clarity of presentation.

faces.²⁹ The remaining peaks in the spectra could not be reliably assigned due to the scarcity of empirical data for the vibrational modes of pentasubstituted aromatic systems.³⁰ We note that the Raman and SERS spectra in this study bear few similarities to those of closely related resorcinarenes,³¹ indicative of the present limitations of Raman spectral assignments based on structural correlations. In the case of tetraarylthiol **2**, a strong SERS signal with a maximum at 255 cm^{-1} and a shoulder between 275 and 300 cm^{-1} is observed. The peak at 255 cm^{-1} can be accounted for by the $\nu_{\text{Au-Cl}}$ stretching mode, which we also observe from 40-nm particles precipitated by NaCl, whereas the broad shoulder at 275–300 cm^{-1} is again likely produced by the $\nu_{\text{Au-S}}$ stretching mode.²⁹ This suggests that nanoparticles encapsulated by **2** are incompletely passivated and have an appreciable concentration of anionic adsorbates on their surfaces, thus making them more difficult to disperse in nonpolar media.

XPS measurements were conducted on **1** and **2** adsorbed onto Au(111) surfaces, which were prepared by soaking

Au substrates in 1 mM EtOH/ CHCl_3 solutions at room temperature (see Experimental Section). These substrates generated weak but discernible signals in the sulfur 2p region, which were calibrated and fitted as $2p_{3/2}$ and $2p_{1/2}$ doublets (see Figure 8). The sulfur-to-gold peak integration ratio for self-assembled monolayers (SAMs) of **1** and **2** was found to be 0.081 and 0.130, respectively. The corresponding molecular surface densities (estimated based on the S/Au ratio of 0.084 found for a ($\sqrt{3} \times \sqrt{3}$) $R30^\circ$ SAM of butanethiol on gold^{24,32}) were determined to be 90 and 57 $\text{\AA}^2/\text{molecule}$. In comparison, molecular cross-sectional areas of Langmuir–Blodgett films of structurally related resorcinarenes have been estimated to be 140–150 $\text{\AA}^2/\text{molecule}$, based on surface pressure–area isotherms.³³ The high surface densities of **1** and **2** suggest that the adsorbed tetrathiols formed either partial multilayers or more tightly packed monolayers than those observed in Langmuir–Blodgett films.

Tetrabenzylthiol **1** produced two sets of S 2p doublets at 161.7 and 163.2 eV, corresponding respectively to binding energies of sulfur atoms covalently bound to gold and weakly bound or unbound organic sulfur.²⁴ The integrated area ratio of 0.84 suggests an average of at least 1.8 bound sulfurs per resorcinarene, assuming monolayer coverage. Partial chemisorption of the thiol groups in **1** would not be surprising, given the geometrical criteria for optimal chemisorption of organothiols onto Au (see below).¹² Other molecules with multiple thiol or sulfide groups have demonstrated similar partial adsorption profiles.^{24,34} In comparison, tetraarylthiol **2** produced essentially one set of S 2p doublets at 163.5 eV. It is possible that the intensity of the bound sulfur peak was too low to be detected above the noise threshold; however, the possibility of very weak Au–S bonding interactions should also be considered. It has been shown in some cases (e.g., sulfides) that sulfur binding to gold can be sufficiently weak that its charge density is unpolarized by adsorption.³⁵ Regardless of the mode of binding, the XPS data clearly indicate the less robust adsorption of **2** to Au relative to **1**.

Previous surface studies have compared the relative stabilities of monodentate phenylthiols and benzylthiols adsorbed onto Au(111), with the latter generally forming more stable and ordered monolayers.³⁶ Differences in stability have been attributed to the bonded sulfurs favoring sp^3 hybridization with a surface–S–C bond angle of approximately 104° ,³⁷ although recent XPS studies of oligophenylthiols indicate little correlation between molecular orientation (as defined by the molecular tilt angle) and bonding.³⁸ This implies that the weak adsorption of tetraarylthiol **2** on Au is due primarily to steric encumbrance of the bridging dioxymethylene units on the macrocyclic headgroup (see Figure 9). Surface bonding may be further frustrated by an obtuse surface–S–C bond angle; molecular models of **2** suggest a minimum angle of 140° , when the molecular axis is oriented along the surface

(32) Hutt, D. A.; Leggett, G. J. *Langmuir* **1997**, *13*, 3055–58.

(33) (a) Moreira, W. C.; Dutton, P. J.; Aroca, R. *Langmuir* **1994**, *10*, 4148–52. (b) Kurita, E.; Fukushima, N.; Fujimaki, M.; Matsuzawa, Y.; Kudo, K.; Ichimura, K. *J. Mater. Res.* **1998**, *8*, 397–403.

(34) Beulen, M. W. J.; Bügler, J.; Lammerink, B.; Geurts, F. A. J.; Biemond, E. M. E. F.; van Leerdam, K. G. C.; van Veggel, F. C. J. M.; Engbersen, J. F. J.; Reinhoudt, D. N. *Langmuir* **1998**, *14*, 6424–29.

(35) Zhong, C. J.; Brush, R. C.; Anderegg, J.; Porter, M. D. *Langmuir* **1999**, *15*, 518–25.

(36) Tao, Y.-T.; Wu, C.-C.; Eu, J.-Y.; Lin, W.-L.; Wu, K.-C.; Chen, C.-h. *Langmuir* **1997**, *13*, 4018–23.

(37) Sellers, H.; Ulman, A.; Shnidman, Y.; Eilers, J. E. *J. Am. Chem. Soc.* **1993**, *115*, 9389–401.

(38) Frey, S.; Stadler, V.; Heister, K.; Eck, W.; Zharnikov, M.; Grunze, M.; Zeysing, B.; Terfort, A. *Langmuir* **2001**, *17*, 2408–15.

(29) (a) Nuzzo, R. G.; Zegarski, B. R.; Dubois, L. H. *J. Am. Chem. Soc.* **1987**, *109*, 733–40. (b) Carron, K. T.; Hurley, L. G. *J. Phys. Chem.* **1991**, *95*, 9979–84. (c) Szafranski, C. A.; Tanner, W.; Laibinis, P. E.; Garrell, R. L. *Langmuir* **1998**, *14*, 3580–89.

(30) Varsányi, G. *Assignments for Vibrational Spectra of Seven Hundred Benzene Derivatives*; John Wiley and Sons: New York, 1974; Vol. 1.

(31) Nissink, J. W. M.; van der Maas, J. H. *Appl. Spectrosc.* **1999**, *53*, 528–39.

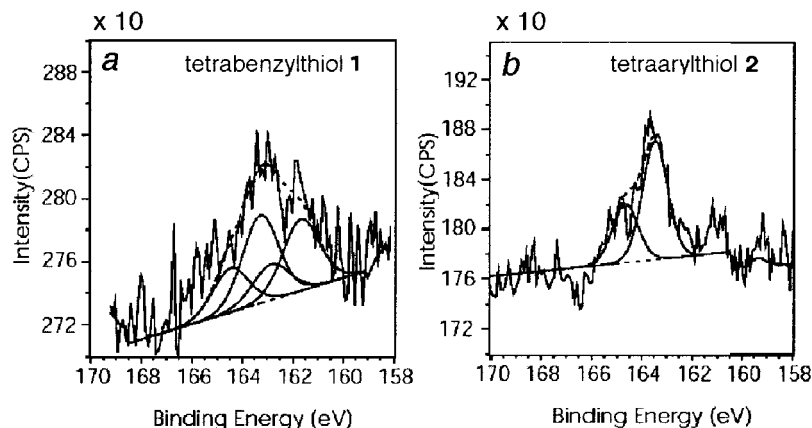


Figure 8. X-ray photoelectron spectra of the sulfur 2p regions of **1** (a) and **2** (b) adsorbed on Au(111) surfaces. Each S 2p peak was fitted as two linked components, $2p_{1/2}$ and $2p_{3/2}$. Peak areas of the $2p_{1/2}$ component were set at half the peak area of the $2p_{3/2}$ component with a fixed peak separation of 1.2 eV. Dashed lines represent the baseline and total curve fits.

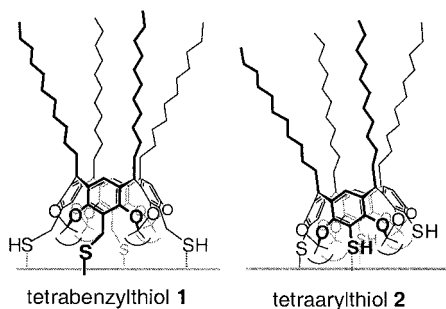


Figure 9. Models of **1** and **2** adsorbed onto Au surfaces, in accord with surface spectroscopic analysis. Dashed bonds represent weak or negligible Au–S orbital overlap.

normal. The sulfurs of **1** are more accessible by comparison, with some of the thiols capable of adopting nearly optimal conformations for bonding to the gold surface.

Conclusions

Tetrathiol resorcinarenes such as **1** and **2** enhance the dispersion and robustness of midnanometer-sized gold particles suspended in organic solvents. Tetrabenzylthiol **1** is clearly a superior dispersant over tetraarylthiol **2** under the conditions examined. SERS and XPS analysis

reveals that **2** adsorbs more weakly and is less effective at passivating gold surfaces than **1**, which affects its ability to partition colloidal gold particles into nonpolar solvents. **2** provides excellent dispersion control of gold nanoparticles at the air–water interface and enables their spontaneous organization into two-dimensional arrays,²³ which indicates that other forces besides steric short-range repulsion are operative during the self-assembly process.

Acknowledgment. The authors gratefully acknowledge the National Science Foundation (BES-0086804 and DMR-9875788), the DARPA Moletronics Program (ONR-00014-99-1-0472), and the U.S. Army TACOM for financial support. This work is also supported by the Integrated Detection of Hazardous Materials (IDHM) Program, a Department of Defense project managed jointly by the Center for Sensing Science and Technology (CSST), Purdue University, and the Naval Surface Warfare Center (NSWC), Crane, Indiana.

Supporting Information Available: Synthetic procedures and chemical characterization for resorcinarenes **1** and **2**. This material is available free of charge via the Internet at <http://pubs.acs.org>.

LA0156107